Zone-axis diffraction study of pressure-induced inhomogeneity in single-crystal $Fe_{1-x}O$

Yang Ding,[a] Haozhe Liu, and Jian Xu
Geophysical Laboratory, Carnegie Institution of Washington, 5251 Broad Branch Road, N.W., Washington, D.C. 20015

Charles T. Prewitt
Department of Geosciences, University of Arizona, Tucson, Arizona 85721

Russell J. Hemley and Ho-kwang Mao
Geophysical Laboratory, Carnegie Institution of Washington, 5251 Broad Branch Road, N.W., Washington, D.C. 20015

(Received 6 April 2005; accepted 6 June 2005; published online 22 July 2005)

A zone-axis synchrotron diffraction study of complex and inhomogeneous $Fe_{1-x}O$ thin single crystal under pressure is presented in this letter. Using this method, four phases are observed to coexist in a single crystal of $Fe_{1-x}O$ at 35 GPa in diamond-anvil cells. One phase has cubic symmetry, whereas the other three phases have not been reported previously and can be interpreted as either orthorhombic or monoclinic. The discovery of multiple phases existing in $Fe_{1-x}O$ indicates that structural inhomogeneity of the sample can be induced under high pressure, a result that has important implications for the high *P-T* behavior of this complex material. Such information is not available using conventional diffraction techniques. © *2005 American Institute of Physics*. [DOI: 10.1063/1.1999016]

Zone-axis diffraction of thin crystals is a powerful technique in transmission electron microscopy, because it provides rich spatial projection symmetry information with a single diffraction pattern.[1] A combination of the projection symmetry information from two or three major zone axes can determine the whole symmetry of the crystal. Since this method was developed for thin crystals and only requires a few diffraction patterns from zone axes of crystals, it is coincidently suitable for application to diamond-anvil-cell-based high-pressure single-crystal research. Normally, symmetry determination and structure refinement by conventional high-pressure single-crystal methods suffer from the limited openings of the cell and the requirement of thin crystals. However, with the zone-axis diffraction method, the high-pressure single-crystal symmetry determination on thin crystals may become easier. Most importantly, the zone-axis diffraction technique is especially suitable for studying multiple phases in one single crystal at high pressure, since no other conventional method is available. This method has seldom been applied with x rays[2,3] because it can only be observed with thin crystals using short-wavelength radiation. With the availability of high-energy x-ray synchrotron sources, there is the prospect of applying this technique in high-pressure diamond-anvil-cell experiments. In this letter, a zone-axis synchrotron diffraction study of complex and inhomogeneous $Fe_{1-x}O$ thin single crystals under pressure is presented to demonstrate the power of this method.

Zone-axis diffraction patterns form when short-wavelength radiation passes through the zone axis of a thin crystal, and it can be regarded as transmission Laue diffraction. Under the single-scattering approximation,[1] the scattering intensity can be expressed as

$$I(K) \propto \left[(N_x N_y N_z V)^2 \frac{\sin^2(\pi N_a \mathbf{K}\cdot\mathbf{a})}{(\pi N_a \mathbf{K}\cdot\mathbf{a})^2} \times \frac{\sin^2(\pi N_b \mathbf{K}\cdot\mathbf{b})}{(\pi N_b \mathbf{K}\cdot\mathbf{b})^2} \times \frac{\sin^2(\pi N_c \mathbf{K}\cdot\mathbf{c})}{(\pi N_c \mathbf{K}\cdot\mathbf{c})^2} \right] |F(\mathbf{K})|^2,$$

where $F(K)$ is the structure factor of the crystal and the rest of the equation is the shape function of the crystal. N_x, N_y, and N_z are the numbers of cells along axes **a**, **b**, and **c** in real space, respectively, while **K** is the scattering vector in reciprocal space. From calculations, if thickness of the $Fe_{1-x}O$ sample is more than 20 μm, then the length of diffraction rods of 220 with 0.4Å wavelength synchrotron x ray can be larger than the excitation error 0.08 $Å^{-1}$, (the distance from Laue diffraction to the flat surface of the detector),[4] and thus can intersect with the detector surface [Fig. 1(a)]. Therefore, partial intensity of the 220 class diffraction can be recorded on a flat two-dimensional detector, even though the Laue

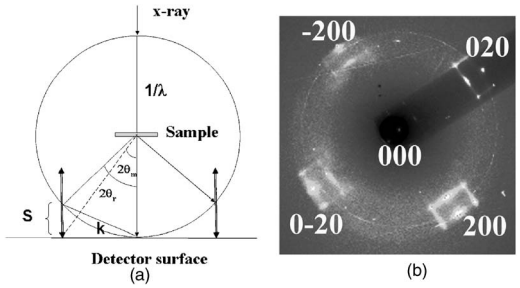

FIG. 1. (a) The construction of Ewald sphere for demonstration of zone-pattern formation. S: The excitation error, which is the length deviating from the Laue condition in reciprocal space ($Å^{-1}$); **k**: Scattering vector in unit $Å^{-1}$. $2\theta_m$: The measured Laue angle by FIT2D; $2\theta_r$; The true diffraction angle; λ; Wavelength of the radiation. (b) A typical ⟨001⟩ zone-axis diffraction pattern of cubic $Fe_{1-x}O$ with synchrotron x ray at 1.0 GPa. The diffuse super-reflections around the main diffraction arise from defect clustering (Refs. 5,6,16).

[a]Author to whom correspondence should be addressed; electronic mail: yding@hpcat.aps.anl.gov

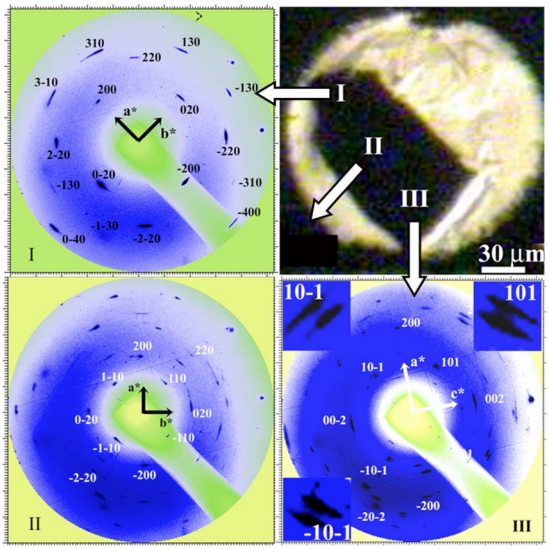

FIG. 2. (Color online) The images of a $Fe_{1-x}O$ single-crystal in a diamond-anvil cell at 35 GPa and the corresponding observed diffraction patterns from Locations I, II, and III of the sample in a diamond-anvil cell. The indexing of each pattern has also been shown. The inserts in Patterns III are the enlarged splitting of diffraction class 101.

condition is not exactly satisfied. The excitation errors, due to the deviation from the Laue condition, can be corrected in *d*-spacing measurement as

$$d_{\text{real}} = d_{\text{measured}} \frac{1}{\cos\,\theta_{\text{measured}}}.$$

$Fe_{1-x}O$, (wüstite), a fundamentally important material in condensed-matter physics, chemistry, and earth science,[7,8] is a rock-salt (B1)-type structured nonstoichiometric iron oxide, and it is commonly incommensurately modulated with long-range ordered defect structure.[5,6] Two high-pressure phase transformations have been reported from previous powder diffraction studies. One is from the ambient pressure B1 phase to a rhombohedral phase near 15–18 GPa at room temperature,[9–11] and the other is from rhombohedral to a B8 (or anti-B8) phase around 74 GPa at 900 K.[12] Here, we re-examined the spatial symmetry changes in $Fe_{1-x}O$ under pressure with zone-axis diffraction method.

The $Fe_{1-x}O$ sample was prepared by cold-pressing reagent-grade hematite (Fe_2O_3) into centimeter-sized pellets. And then, the hematite pellets were held for ~24 h at 1200 °C and 10-11 bars f_{O_2} in a CO/CO_2 gas-mixing furnace.[13] The cell parameter of the $Fe_{1-x}O$ was measured by x-ray diffraction to be $a=4.303(2)$Å, corresponding to $Fe_{0.93}O$.[14] High pressures were generated between two gem-quality single-crystal diamonds with 400 μm culets in a symmetric diamond cell. One single crystal of $Fe_{1-x}O$ about $70\times35\times20$ μm^3, cut along the {001} plane, was placed into a 120 μm hole that was drilled in a 45 μm thick stainless-steel gasket. One small ruby chip was added as a pressure calibration standard, and a 4:1 methanol–ethanol mixture was used as the pressure medium. The diffraction experiments were performed at beamline 16-IDB, High-Pressure Collaborative Access Team of the Advanced Photon Source, Argonne National Laboratory. The diamond-anvil cell was mounted on a stage that could be rotated up to 10° around the vertical and horizontal axes for alignment purposes. Zone-axis diffraction patterns were taken along the ⟨001⟩ zone axis of cubic $Fe_{1-x}O$ and recorded with a Mar345 image plate. Diffraction data were analyzed with the FIT2D program.[15]

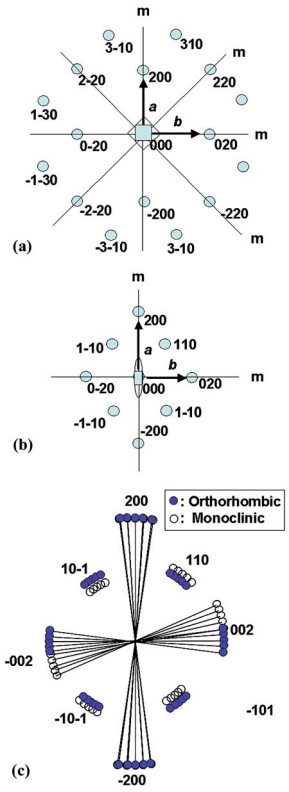

FIG. 3. The calculated diffraction patterns for the four phases of the sample. (a) Simulation of diffraction pattern for Phase I using symmetry Fm-3m along ⟨001⟩ zone axis. (b) Simulation of diffraction pattern for Phase II using symmetry Cmmm along ⟨001⟩ zone axis. (c) Simulation of diffraction patterns for Phase III (Cmmm) and Phase IV ($C2/m$) along [010] zone axes. The two phases have same lattice parameter a and c, but the monoclinic Phase IV has β lattice parameter as 92 ° . The solid circle stands for the orthorhombic phase and the open circle stands for the monoclinic phase. Four of the same diffraction patterns with small offset in β angles of the monoclinic phase are exaggerated in order to clearly show the splitting of 110 diffraction class. m: Mirror plane; ◇: Four-fold-rotation axis. ⬭: Two-fold-rotation-axis.

The measurements were carried out up to 35 GPa with about a 2 GPa increase in pressure at each step, and a typical ⟨001⟩ zone-axis diffraction pattern from cubic $Fe_{1-x}O$ at low pressure is displayed in Fig. 1(b). A long-range defect cluster order-disorder transition was observed around 14 GPa from the incommensurate superstructure reflections. Then, the cubic $Fe_{1-x}O$ transformed into the rhombohedral phase after 19.8 GPa. The detailed description of the results below 25 GPa will be reported elsewhere.[16] Surprisingly, the rhombohedral phase in turn transformed into four phases at 31.9 GPa. Diffraction patterns from three locations—I, II, III—of the sample indicate four phases coexisting in the single crystal pattern of $Fe_{1-x}O$ taken at 35 GPa are displayed in Fig. 2.

The diffraction pattern from Phase I of the sample shows a projection symmetry of $4mm1_R$,[4] which is the same as that of the phase below 19.8 GPa and suggests a cubic symmetry (Fig. 2). The lattice parameter $a=4.100$ Å was obtained from fitting the pattern. The appearance of 310 class diffraction, which should be absent in the B1 structure, probably arises from structure defects. The simulation of the diffraction patterns using $Fm3m$ along the ⟨001⟩ zone axis is shown in Fig. 3(a). The highest projection-diffraction symmetry from Phase II shown in Fig. 2 is $2mm1_R$.[4] Since no other higher

symmetry zone-axis pattern was obtained due to the limited opening angle of the diamond-anvil cell, it is difficult to uniquely determine the space group of the phase. Since the pattern was taken along the highest symmetry zone-axis of cubic $Fe_{1-x}O$, it is possible that the zone-axis pattern of Phase II, transformed from a nearly cubic phase, still bears the highest symmetries. If so, the symmetry of the zone-axis pattern $2mmm1_R$ indicates that the symmetry of Phase II is not higher than orthorhombic. Considering that the principal **a**,**b** axes of Phase II are parallel to ⟨220⟩ of cubic Phase I, Phase II is most likely structurally coherent with Phase I. Symmetries lower than orthorhombic may introduce tilt phase boundaries which may increase the free energy of the system and not favor the formation of the new phases. Indexing according to orthorhombic symmetry shows $h+k=2n$, or $h+k+l=2n$, indicating a *C* or *I* lattice. Accordingly, the highest-symmetry space group that can yield the same diffraction patterns is *Cmmm* or *Immm*. The measured lattice parameters *a* and *b* are 4.618Å and 4.970Å, respectively. With the assumption that Phase II has the same stoichiometry as that of cubic $Fe_{1-x}O$ (Fe:O close to 1:1), and the Fe ions are octahedrally coordinated by oxygen atoms, then, *Cmmm* structure has a closer structural relationship to the B1 structure. The simulation of the diffraction pattern from Phase II using symmetry *Cmmm* along the ⟨001⟩ zone axis is shown Fig. 3(b). Since the lattice parameters *a* and *b* of Phase II are larger than that of cubic Phase I, *c* must be smaller than 3.00Å, thus ensuring a volume decrease at phase the transformation.

The diffraction pattern from Location III of the sample has a symmetry similar to that of Phase II (Fig. 2), but it contains two phases shown by the splitting of some diffraction. If we treat the splitting diffraction as the same diffraction, then the diffraction from Location III has symmetry similar to that of Phase II, and thus can be indexed using orthorhombic symmetry *Cmmm*. Two lattice parameters of the phases are measured as $a=2.932$ Å and $c=4.062$ Å, but lattice parameter *b* cannot yet be determined. However, the 110 diffraction class splits by 0.26° in diffraction angle, indicating that there are two phases (Phases III and IV), and one phase is monoclinic. The two phases have the same lattice *a* and *c* but differ in β angle; the β angle of Phase IV is 92° if Phase III is treated as orthorhombic according to calculations.[17] The structure of Phase III might be similar to that of Phase II because they have similar diffraction patterns, but they have different lattice parameters. Since Phases III and IV differ only by 2° in the β parameter, then symmetry C2/m can be the best choice for Phase IV since it is the closest monoclinic symmetry to *Cmmm* of Phase III and also is able to produce the same diffraction pattern as that from measurement along the [010] zone axis. The simulations of the diffraction pattern from Phases III and IV are shown in Fig. 3(c). In the simulations, four of the same diffraction patterns with a few degrees difference in orientation are overlaid for each phase in order to simulate the mosaic spread. It can be noted that the splitting of diffraction class 200 is smeared out by the mosaic spread. Upon the release of pressure, Phases II and III are quenchable to ambient condition. But Phase IV disappears at 13.8 GPa which suggests another phase transition from the monoclinic to the orthorhombic phase. It is noteworthy that some diffraction spots in Phases II and III arise from still other structures, but these cannot yet be identified since their zone axes are not parallel to the x-ray beam.

The discovery of multiple phases existing in $Fe_{1-x}O$ indicates that high pressure can induce structural inhomogeneity of the sample. The origin of such pressure-induced inhomogeneity likely results from two mechanisms. One is that the known defect clusters[5,6] change their geometry and distribution and develop into complex two-dimensional structural defects in different domains, which in turn trigger multiple phase transformations under pressure. The stress resulting from the coherent structures may also have an influence on the lattice parameters and structures of coherent phases. The second mechanism is that compositional fluctuations, which occur during synthesis,[18] develop into different phases upon compression. The observed complexity also indicates that $Fe_{1-x}O$ cannot be treated simply as an Fe–O binary system, but a quaternary system including ferrous and ferric iron, oxygen, and vacancies. Consequently, the discovery of pressure-induced inhomogeneity of $Fe_{1-x}O$ may result in the reconsideration of the interpretation of its electronic/magnetic properties measured under high pressure. Through this study of $Fe_{1-x}O$, the new diamond-anvil-cell-based zone-axis single-crystal technique is shown to be a powerful tool for investigating inhomogeneous samples at high pressures.

The authors are grateful to S. Jacobsen for kindly providing the single-crystal sample and to M. Somayazulu for helpful discussions. They also appreciate M. Phillips for help with the manuscript. This work was supported by DOE/NNSA (CDAC), NSF, and W. M. Keck Foundation.

[1] P. Buseck, J. M. Cowley, and L. Eyring, *High-Resolution Transmission Electron Microscopy and Associated Techniques* (Oxford University Press, New York, 1988).
[2] H. Tajiri, O. Skata, and T. Takahashi, Appl. Surf. Sci. **234**, 403 (2004).
[3] M. Holt, Z. Wu, H. Hong, P. Zschack, P. Jemian, J. Tischler, H. Chen, and T.-C. Chiang, Phys. Rev. Lett. **87**, 255501-1 (2001).
[4] D. B. Williams and C. B. Carter, *Transmission Electron Microscopy: A Textbook For Materials Science* (Plenum, New York, 1996).
[5] F. Koch and J. B. Cohen, Acta Crystallogr., Sect. B: Struct. Crystallogr. Cryst. Chem. **25**, 275 (1969).
[6] T. R. Welberry and A. G. Christy, Phys. Chem. Miner. **24**, 24 (1997).
[7] R. E. Cohen, I. I. Mazin, and D. G. Issak, Science **275**, 654 (1997).
[8] C. G. Shull, W. A. Strauser, and E. O. Wollan, Phys. Rev. **83**, 333 (1951).
[9] H. K. Mao, J. Shu, Y. Fei, J. Hu, and R. J. Hemley, Phys. Earth Planet. Inter. **96**, 135 (1996).
[10] T. Yagi, T. Suzuki, and S.-i. Alkimoto, J. Geophys. Res. **90**, 8784 (1985).
[11] J. Shu, H. K. Mao, J. Hu, Y. Fei, and R. J. Hemley, N. Jb, Miner. Abh **172**, 309 (1998).
[12] Y. Fei and H. K. Mao, Science **266**, 1678 (1994).
[13] Y. Ding J. Xu, C. T. Prewitt, R. J. Hemley, H. K. Mao, A. Cowan, J. Zhang, J. Qian, S. C. Vogel, and Y. Zhao, Appl. Phys. Lett. **86**, 052505 (2005).
[14] B. Simons, Year Book - Carnegie Inst. Washington **79**, 376 (1980).
[15] A. P. Hammersley, S. O. Svensson, M. Hanfland, A. N. Fitch, and D. Häusermann, High Press. Res. **14**, 235 (1996).
[16] Y. Ding, O. Degtyareva, H. Liu, M. Somayazulu, Y. Meng, J. Xu, C. T. Prewitt, R. J. Hemley and H.-k. Mao, (unpublished).
[17] For monoclinic crystal, $d_{101}=1/\sqrt{(1/a^2+1/c^2+2/ac)\cos\beta/\sin^2\beta}$. Since the d_{101} of monoclinic Phase IV differs from that of orthorhombic Phase III by about 0.26° in diffraction angle, (equal to 0.038Å in real space), the calculated β lattice parameter for Phase IV is about 92° if the β of Phase III is 90°; the two phases have the same lattice parameter *a* and *c*.
[18] B. Andersson and J. O. Sletnes, Acta Crystallogr., Sect. A: Cryst. Phys., Diffr., Theor. Gen. Crystallogr. **33**, 268 (1977).